Supporting information

Photocatalytic CO_2 reduction with iron porphyrin catalysts and anthraquinone dyes

Huiqing Yuan,[*a,b] Yuanhai Yu,[b] Shuang Yang,[b] Qinqin Lei,[b] Zhiwei Yang,[b] Bang Lan,[*a] and Zhiji Han[*b]

[a] School of Chemistry and Environment, Jiaying University, Meizhou, Guangdong 514015, China. E-mail: yuanhq3@mail2.sysu.edu.cn; jyulb6@163.com

[b] MOE Key Laboratory of Bioinorganic and Synthetic Chemistry, School of Chemistry, Sun Yat-sen University, Guangzhou 510275, China. hanzhiji@mail.sysu.edu.cn

Table of Contents

General Consideration

All solvents and reagents were procured from commercial sources and utilized as received. BIH was synthesized according to the methods of literature.[1] UV-visible absorption spectra were acquired using a Thermo Scientific GENESYS 50 UV-visible spectrophotometer. Elemental analysis was obtained at an Elementar Vario EL analyzer. Dynamic light scattering experiments were conducted with a Brookhaven Elite Sizer zata-potential and particle size analyzer. ^{1}H NMR spectra were recorded with a Bruker advance III 400 MHz NMR instrument.

Synthesis of 5,10,15,20-tetrakis(4'-bromo-2',6'-dimethoxyphenyl)porphyrin

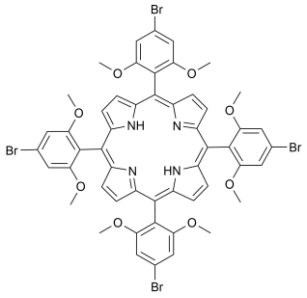

5,10,15,20-tetrakis(4'-bromo-2',6'-dimethoxyphenyl)porphyrin was synthesized following a modified literature procedure.[2] Initially, a mixture of 4'-bromo-2',6' dimethoxybenzaldehyde (1.475 g, 6.02 mmol) and pyrrole (0.419 mL, 6.02 mmol) in $CHCl_3$ (600 mL) was subjected to N_2 degassing for a minimum of 20 minutes. Then, boron trifluoride diethyl etherate ($BF_3 \cdot OEt_2$, 0.228 mL, 0.87 mmol) was added dropwise using a syringe. The solution was stirred at ambient temperature under N_2 atmosphere in darkness for 1.5 hours, after which 2,3-dichloro-5,6-dicyano-1,4-benzoquinone (DDQ, 1.02 g, 4.51 mmol) was incorporated. Stirring was continued for an additional 1.5 hours at reflux. Upon cooling to room temperature, the reaction mixture was treated with triethylamine (1 mL) to neutralize any residual acidity. Subsequent removal of the solvent yielded a black solid, which was purified via column chromatography on silica gel using dichloromethane (CH_2Cl_2) as the eluent. The purification process resulted in the isolation of 5,10,15,20-tetrakis(4'-bromo-2',6'-dimethoxyphenyl)porphyrin as a purple powder (390 mg, 22% yield). ^{1}H NMR (400 MHz, $CDCl_3$): δ 8.67 (s, 8H), 7.14 (s, 8H), 3.50 (s, 24H), -2.62 (s, 2H). HRMS (m/z): $[M + H]^+$ Calcd. for $C_{52}H_{42}N_4O_8Br_4$ 1170.97680; found, 1170.97688.

Synthesis of 5,10,15,20-tetrakis(4'-bromo-2',6'- dihydroxyphenyl)porphyrin

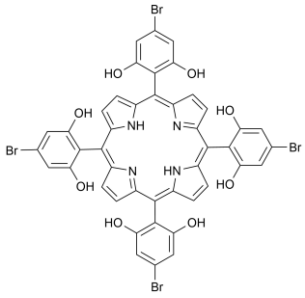

To a stirred solution of 5,10,15,20-tetrakis(4’-bromo-2’,6’-dimethoxyphenyl)porphyrin (300 mg, 0.256 mmol) in anhydrous dichloromethane (20 mL), boron tribromide (BBr_3, 3.0 mL, 31.14 mmol) was added at 0 °C under a nitrogen atmosphere. The mixture, which turned green upon addition, was stirred at room temperature for 72 hours. Subsequently, water (10.0 mL) was carefully added to the reaction mixture at 0 °C, followed by stirring for an additional 40 minutes. The reaction was neutralized with saturated $NaHCO_3$ solution until the pH of the aqueous phase reached approximately 7. Ethyl acetate (50 mL) was then introduced, and the organic layer was separated and washed with water (3 × 50 mL). After solvent evaporation, the residue underwent purification by column chromatography on silica gel, eluting with a 2:1 mixture of ethyl acetate and dichloromethane, to afford 5,10,15,20-tetrakis(4’-bromo-2’,6’-dihydroxyphenyl)porphyrin as a purple powder (237 mg, 87.4% yield). ^{1}H NMR (400 MHz, CD_3OD): δ 8.90 (s, 8H), 6.98 (s, 8H). HRMS (m/z): $[M + H]^+$ Calcd. for $C_{44}H_{26}N_4O_8Br_4$ 1058.85160; found, 1058.85308.

Synthesis of chloro iron(III) 5,10,15,20-tetrakis(4’-bromo-2’,6’-dihydroxyphenyl)porphyrin (Fe1)

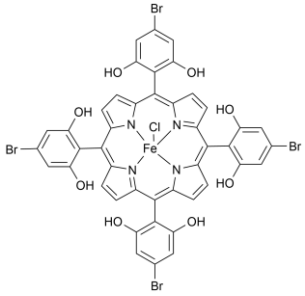

Fe1 was synthesized by combining 5,10,15,20-tetrakis(4’-bromo-2’,6’-dihydroxyphenyl)porphyrin (200 mg, 0.189 mmol), and iron(II) chloride tetrahydrate ($FeCl_2 \cdot 4H_2O$, 540 mg, 2.7 mmol) in anhydrous methanol. The reaction mixture was heated at 50 °C for 48 hours under a nitrogen atmosphere. Following solvent removal, the resultant brown solid was dissolved in ethyl acetate (50 mL) and treated with 1.2 M HCl (50 mL), stirred for 4 hours. The organic layer was separated and washed with saturated NaCl solution until a neutral pH was achieved. Following the removal of the organic solvent through rotary evaporation, the crude product was subjected to purification by column chromatography on silica gel, using ethyl acetate as the eluent, to yield **Fe1** as a brown

solid. Subsequently, **Fe1** was dissolved in ethyl acetate, and the crystallization was induced through the slow diffusion of petroleum ether as the top layer, leading to the formation of plate-like rectangular single crystals. However, the quality of the crystals was poor, making them unsuitable for measurement. After collecting the single crystals, they were redissolved in ethyl acetate (50 mL), with the addition of 50 mL of 1.2 M HCl, and the mixture was stirred continuously for one day. Following the completion of the reaction, the solvent was evaporated under reduced pressure, and the resultant product was dried in a vacuum (130 mg, 60% yield). HRMS (m/z): $[M\text{-}Cl]^+$ Calcd. for $C_{44}H_{24}FeN_4O_8$ 1111.76306; found, 1111.76404. Elemental analysis Calcd. for $C_{52}H_{46}Br_4ClFeN_4O_{15}$ (**Fe1**·$3H_2O$·2EA): C, 45.33%; H, 3.37%; N, 4.07%. Found: C, 45.02%; H, 3.41%; N, 4.36%.

Synthesis of 5,10,15,20-tetrakis(2',6'-dimethoxy-4'-methylphenyl)porphyrin

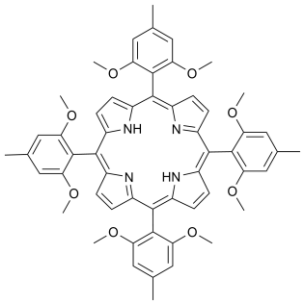

5,10,15,20-tetrakis(2',6'-dimethoxy-4'-methylphenyl)porphyrin was synthesize following a modified literature procedure.[2] Initially, a mixture of 2,6-dimethoxy-4-methylbenzaldehyde (1.084 g, 6.02 mmol) and pyrrole (0.419 mL, 6.02 mmol) in chloroform (600 mL) was subjected to N_2 degassing for a minimum of 20 minutes. Then, boron trifluoride diethyl etherate ($BF_3{\cdot}OEt_2$, 0.228 mL, 0.87 mmol) was added dropwise using a syringe. The solution was stirred at ambient temperature under N_2 atmosphere in darkness for 1.5 hours, after which 2,3-dichloro-5,6-dicyano-1,4-benzoquinone (DDQ, 1.02 g, 4.51 mmol) was incorporated. Stirring was continued for an additional 1.5 hours at reflux. Upon cooling to room temperature, the reaction mixture was treated with triethylamine (1 mL) to neutralize any residual acidity. Subsequent removal of the solvent yielded a black solid, which was purified via column chromatography on silica gel using dichloromethane as the eluent. The purification process resulted in the isolation of 5,10,15,20-tetrakis(2',6'-dimethoxy-4'-methylphenyl)porphyrin as a purple powder (180 mg, 13% yield). ^1H NMR (400 MHz, $CDCl_3$): δ 8.67 (s, 8H), 6.79 (s, 8H), 3.47 (s, 24H), 2.68 (s, 12H), -2.51 (s, 2H). HRMS (m/z): $[M + H]^+$ Calcd. for $C_{56}H_{54}N_4O_8$ 911.40144; found, 911.40090.

Synthesis of 5,10,15,20-tetrakis(2',6'-dihydroxy-4'-methylphenyl)porphyrin

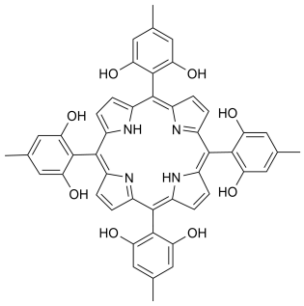

To a stirred solution of 5,10,15,20-tetrakis(2',6'-dimethoxy-4'-methylphenyl)porphyrin (100 mg, 0.11 mmol) in anhydrous dichloromethane (20 mL), boron tribromide (BBr_3, 2.0 mL, 20.76 mmol) was added at 0 °C under a N_2 atmosphere. The mixture, which turned green upon addition, was stirred at room temperature for 72 hours. Subsequently, water (10.0 mL) was carefully added to the reaction mixture at 0 °C, followed by stirring for an additional 40 minutes. The reaction was neutralized with saturated $NaHCO_3$ solution until the pH of the aqueous phase reached approximately 7. Ethyl acetate (50 mL) was then introduced, and the organic layer was separated and washed with water (3 × 50 mL). After solvent evaporation, the residue underwent purification by column chromatography on silica gel, eluting with a 2:1 mixture of ethyl acetate and dichloromethane, to afford 5,10,15,20-tetrakis(2',6'-dihydroxy-4'-methylphenyl)porphyrin as a purple powder (75 mg, 85% yield). ^{1}H NMR (400 MHz, CD_3OD): δ 8.89 (s, 8H), 6.65 (s, 8H), 2.54 (s, 12H). HRMS (m/z): $[M + H]^+$ calcd for $C_{48}H_{38}N_4O_8$ 799.27624; found, 799.27672.

Synthesis of chloro iron(III) 5,10,15,20-tetrakis(2',6'-dihydroxy-4'-methylphenyl)porphyrin (Fe3)

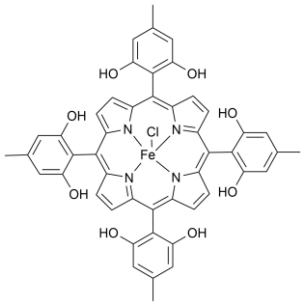

Fe3 was synthesized by combining 5,10,15,20-tetrakis(2',6'-dihydroxy-4'-methylphenyl) porphyrin (50 mg, 0.063 mmol), and $FeCl_2 \cdot 4H_2O$ (180 mg, 0.9 mmol) in anhydrous methanol. The reaction mixture was heated at 50 °C for 48 hours under a nitrogen atmosphere. Following solvent removal, the resultant brown solid was dissolved in ethyl acetate (30 mL) and treated with 1.2 M HCl (30 mL), stirred for 4 hours. The organic layer was separated and washed with saturated NaCl solution until a neutral pH was achieved. Following the removal of the organic solvent through rotary evaporation, the crude product was subjected to purification by column chromatography on silica gel, using ethyl acetate as the eluent, to yield **Fe3** as a brown solid. Subsequently, **Fe3** was dissolved in ethyl

acetate, and the crystallization was induced through the slow diffusion of petroleum ether as the top layer. However, the resulting crystals were too small to allow for single-crystal analysis. Subsequently, the fine crystals were collected and dissolved in ethyl acetate (30 mL). with the addition of 30 mL of 1.2 M HCl, and the mixture was stirred continuously for one day. Following the completion of the reaction, the solvent was evaporated under reduced pressure, and the resultant product was dried in a vacuum (45 mg, 80% yield). HRMS (m/z): $[M\text{-}Cl]^+$ calcd for $C_{44}H_{24}FeN_4O_8$ 852.18771; found, 852.18781. Elemental analysis Calcd. for $C_{66}H_{76}ClFeN_4O_{15}$ (**Fe3**·H_2O·3EA·C_6H_{14}): C, 63.08%; H, 6.01%; N, 4.46%. Found: C, 63.16%; H, 6.42%; N, 4.18%.

Synthesis of chloro iron(III) 5,10,15,20-tetrakis(2',6'-dihydroxy)porphyrin (Fe2)

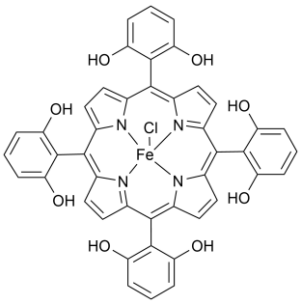

The synthesis of **Fe2** was conducted based on previously reported literature, with modifications to the original procedure.[2] The purified **Fe2** was dissolved in ethyl acetate, followed by an attempt at recrystallization through slow diffusion with petroleum ether as the overlaying solvent. Unfortunately, this process did not yield any crystals. Consequently, the resulting powder was collected and redissolved in ethyl acetate (30 mL). Subsequently, 1.2 M HCl (30 mL) was added to the solution, which was stirred continuously for one day. After the reaction was completed, the solvent was removed under reduced pressure by rotary evaporation, and the product was dried under vacuum. Elemental analysis Calcd. for $C_{56}H_{62}ClFeN_4O_{19}$ (**Fe2**·5H_2O·3EA): C, 61.42%; H, 5.71%; N, 5.12%. Found: C, 61.47%; H, 5.57%; N, 5.49%.

Photocatalytic CO_2 Reduction. Photocatalytic reactions were performed in sealed glass vials (headspace: 51.8 mL) equipped with rubber stoppers and subjected to magnetic stirring. The reaction mixture (5.0 mL) was purged with carbon dioxide (CO_2) for 25 minutes before exposure to blue LED illumination (λ = 450 nm, PCX-50C, Beijing Perfectlight Technology Co., Ltd. Please refer to our previous report for the emission spectrum of the blue LED light source[3]). Gaseous products were quantitatively analyzed using a Shimadzu GC-2014 gas chromatograph, which was fitted with Shimadzu Molecular Sieve 13X 80/100 (3.2 mm × 2.1 mm × 3.0 m) and Porapak N (3.2 mm × 2.1 mm × 2.0 m) columns. Detection of H_2 was facilitated by a thermal conductivity detector (TCD), while CO and other hydrocarbons were detected using a flame ionization detector

(FID) coupled with a methanizer. Nitrogen served as the carrier gas. The chromatographic oven was maintained at 60 °C, with the TCD detector and injection port temperatures held at 100 °C and 200 °C, respectively.

Cyclic Voltammetry. Cyclic voltammetry (CV) experiments were conducted using a CHI-760E electrochemical workstation within a single-compartment cell equipped with a glassy carbon electrode (3 mm diameter) as the working electrode, a platinum auxiliary electrode, and a saturated calomel electrode (SCE) as the reference electrode. The electrolyte consisted of 0.1 M tetrabutylammonium hexafluorophosphate dissolved in DMF. Prior to measurements, solutions were subjected to N_2 or CO_2 purging for 30 minutes to ensure deoxygenation. All potentials reported herein are referenced to the SCE.

Fluorescence Quenching. A solution containing the designated photosensitizer was degassed by nitrogen for 15 minutes in a hermetically sealed quartz cuvette with a septum cap. After the degassing process, BIH was introduced into the nitrogen-saturated solution of the photosensitizer. The lifetimes of **PS1** and **PS2** at 472 nm were determined using a laser spectroscopy instrument (FLS 980, Edinburgh Instruments). The quenching rate constant (k_q) was calculated by the Stern-Volmer equation (1):

$$I_0/I \text{ or } \tau_0/\tau = 1 + k_q \times \tau_0 \times [Q] \qquad (1)$$

where I_0 and I represent the fluorescence intensity of the photosensitizer in the absence and presence quencher, k_q is the quenching rate constant; τ_0 and τ is the lifetime of the photosensitizer in the absence and presence of the quencher, $[Q]$ is the concentration of quencher.

Quantum Yield Measurement. The differential light absorption by photosensitizer was determined by comparing the power of light transmitted through a control solution (containing catalyst and BIH) with that through the test sample (containing photosensitizer, catalyst, and BIH). The average irradiance, P (W/cm^2), was quantified using a FZ-A Power meter from Beijing Normal University Optical Instrument Co. Blue monochromatic light at 450 nm was generated by a LED light source (model PCX-50C, Beijing Perfectlight Technology Co., Ltd.). The quantum yield for the photocatalytic reduction of CO_2 to CO, following exposure to 450 nm light, was calculated employing the subsequent equation:

$$\Phi_{CO} = \frac{2 \times number\ of\ the\ CO\ molecules}{number\ of\ incident\ photons} \times 100\% \quad (2)$$

that is,

$$\Phi_{CO} = \frac{2 \times n(CO)}{I} \times 100\% \qquad (3)$$

where n(CO) is the number of molecules of CO produced, I is the number of incident photons; the calculation formula of the incident photon number I is as follows:

$$I = PSt\frac{\lambda}{hc} \qquad (4)$$

where S is the incident irradiation area (S = 6.33 cm^2), t is the irradiation time, λ is the incident wavelength, h is the Plank constant (6.626× 10^{-34} J·s), c is the speed of light (3×10^8 m s^{-1}).

$$\Phi = \frac{2 \times n(CO) \times N_A}{PSt \times \frac{\lambda}{hc}} \times 100\% \qquad (5)$$

where N_A is the Avogadro constant (6.02×10^{23} mol^{-1}).

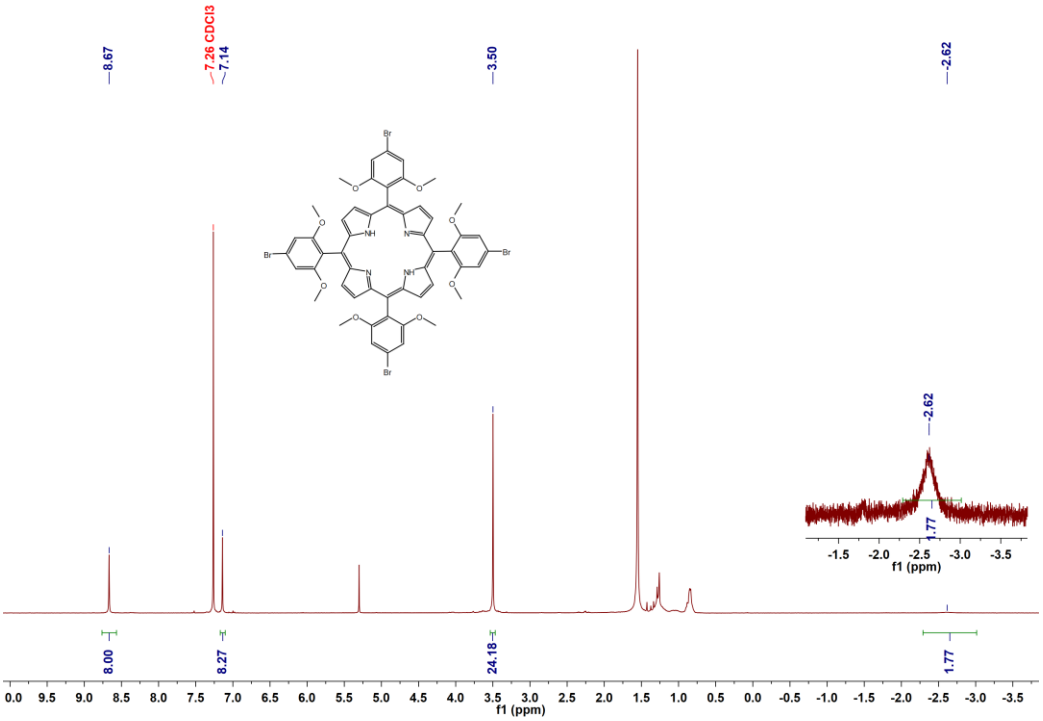

Fig. S1 ^{1}H NMR spectrum of 5, 10, 15, 20-tetrakis(4'-bromo-2',6'-dimethoxyphenyl)-21H,23H-porphyrin in $CDCl_3$.

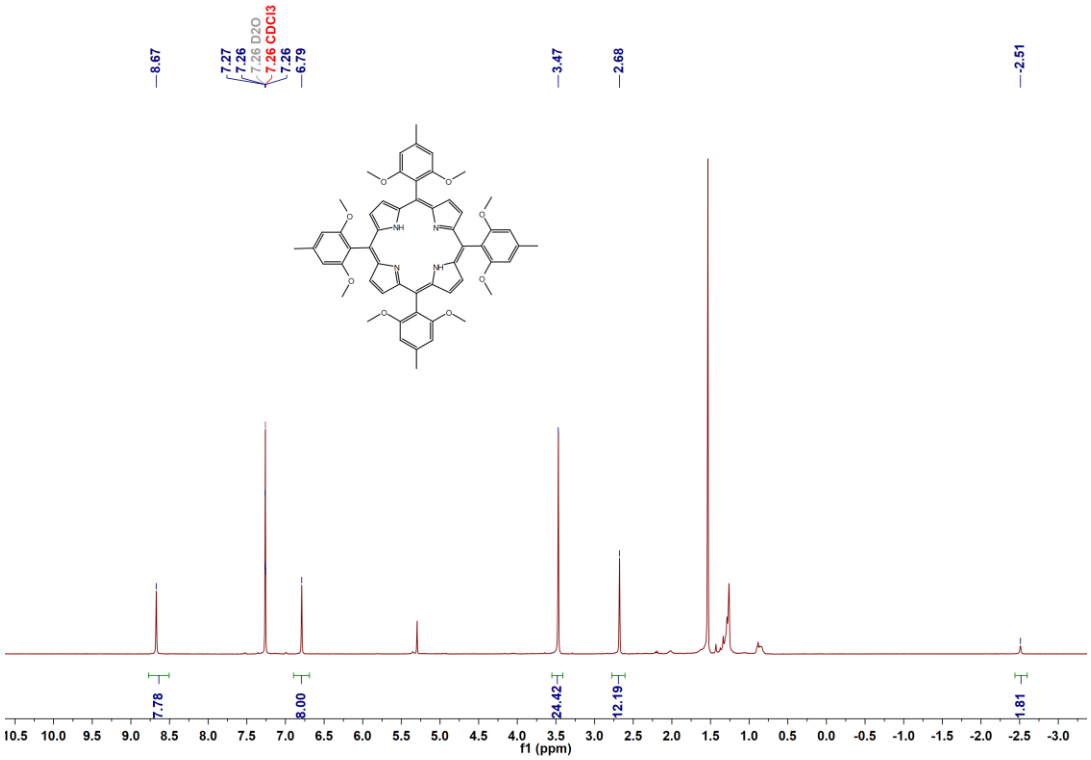

Fig. S2 ^{1}H NMR spectrum of 5, 10, 15, 20-tetrakis(2',6'-dimethoxy-4'-methylphenyl)-21H,23H-porphyrin in $CDCl_3$.

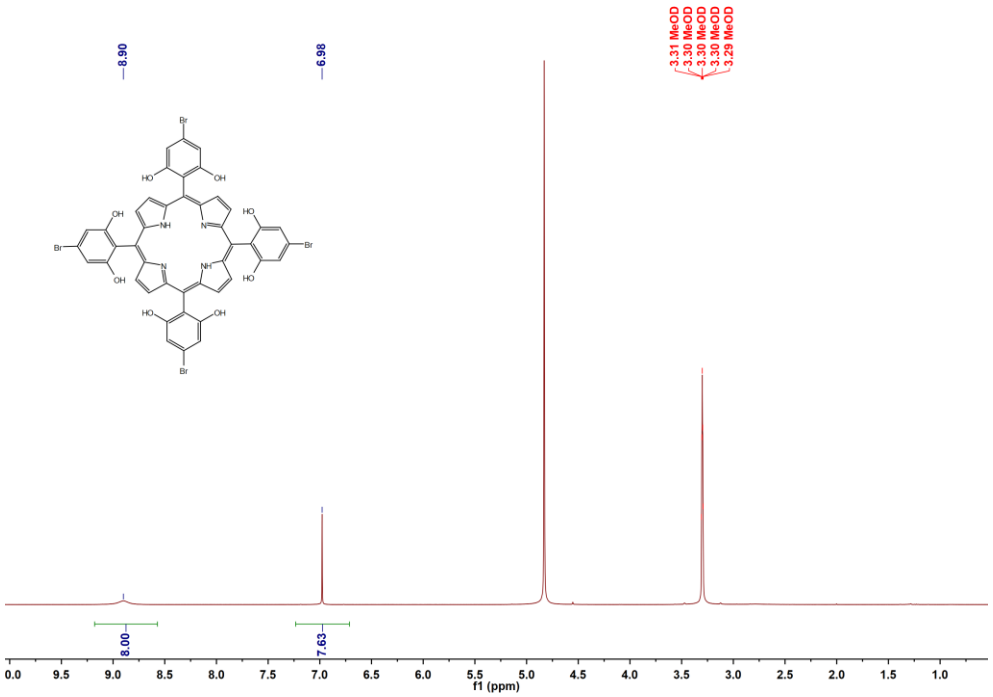

Fig. S3 ^{1}H NMR spectrum of 5, 10, 15, 20-tetrakis(4'-bromo-2',6'-dihydroxyphenyl)-21H,23H-porphyrin in CD_3OD.

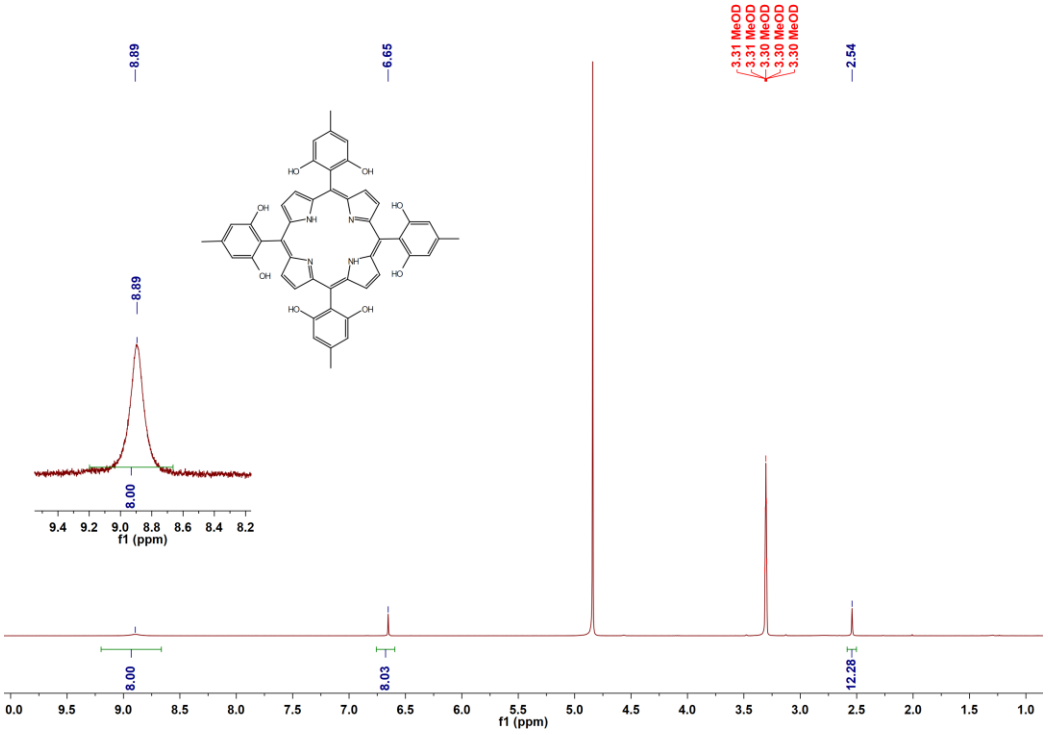

Fig. S4 ^{1}H NMR spectrum of 5, 10, 15, 20-tetrakis(2',6'-dihydroxy-4'-methylphenyl)-21H,23H-porphyrin in CD_3OD.

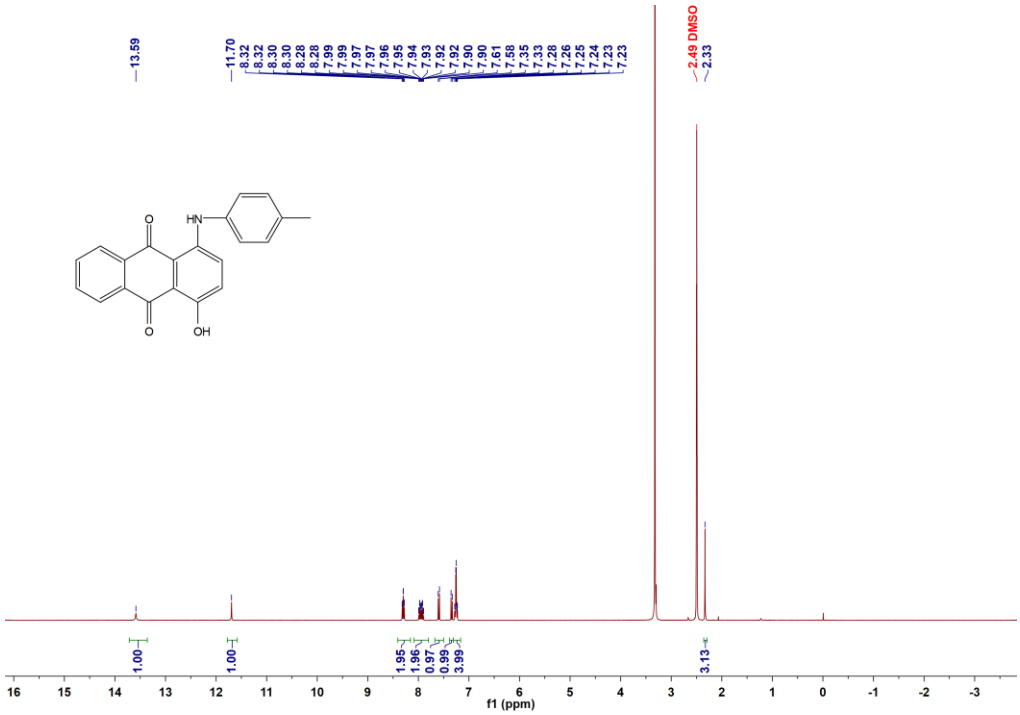

Fig. S5 ^{1}H NMR spectrum of **PS1** in DMSO-d_6.

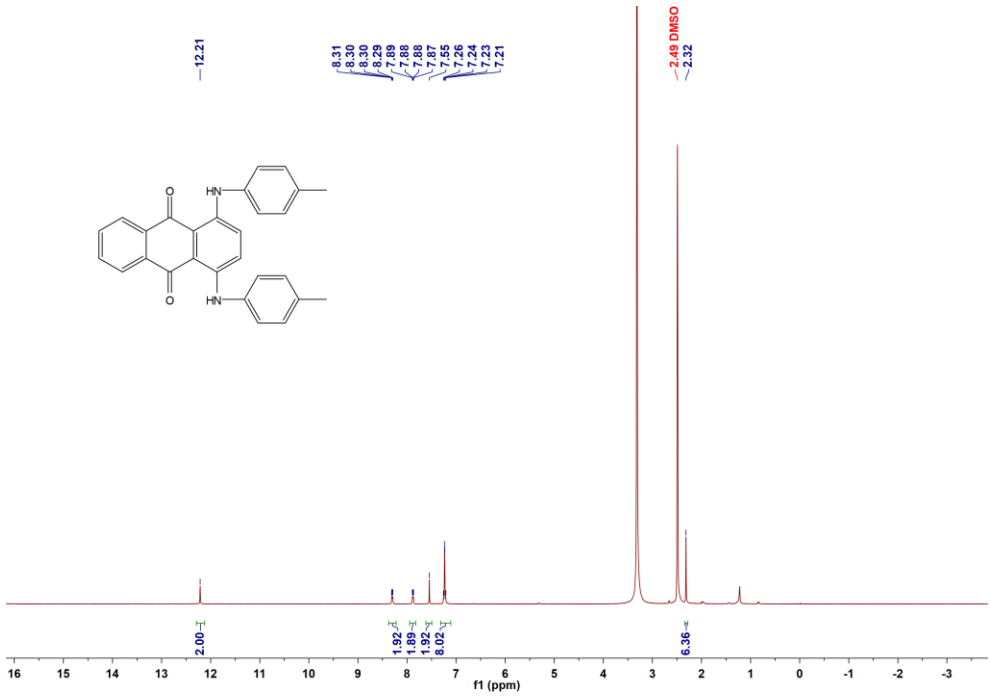

Fig. S6 ^{1}H NMR spectrum of **PS2** in DMSO-d_6.

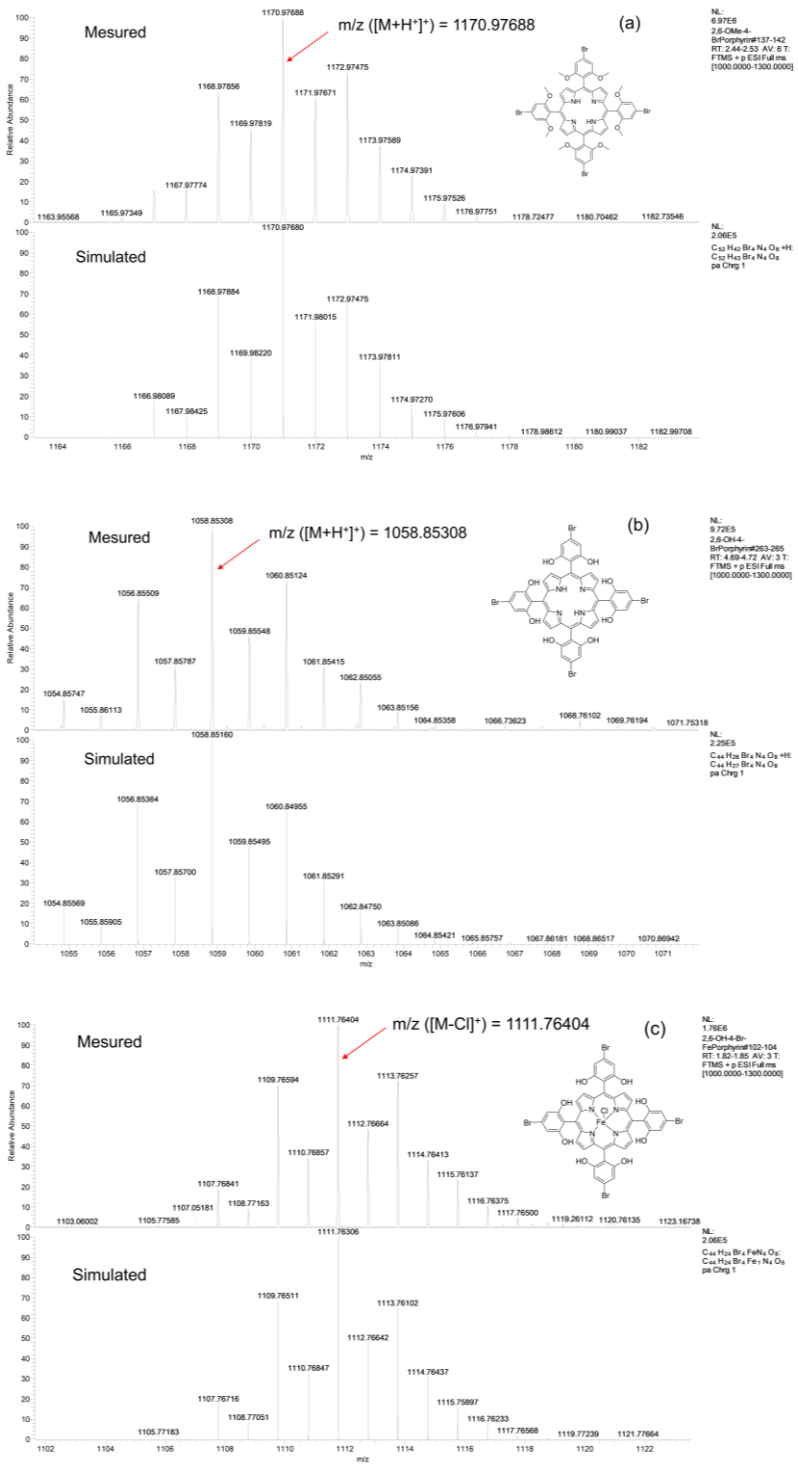

Fig. S7 HRMS spectra of 5, 10, 15, 20-tetrakis(4'-bromo-2',6'-dimethoxyphenyl)porphyrin (a); 5, 10, 15, 20-tetrakis(4'-bromo-2',6'-dihydroxyphenyl)porphyrin (b); and chloro iron (III) 5, 10, 15, 20-tetrakis(4'-bromo-2',6'-dihydroxyphenyl) porphyrin (**Fe1**) (c) in CH_3OH(positive ion mode).

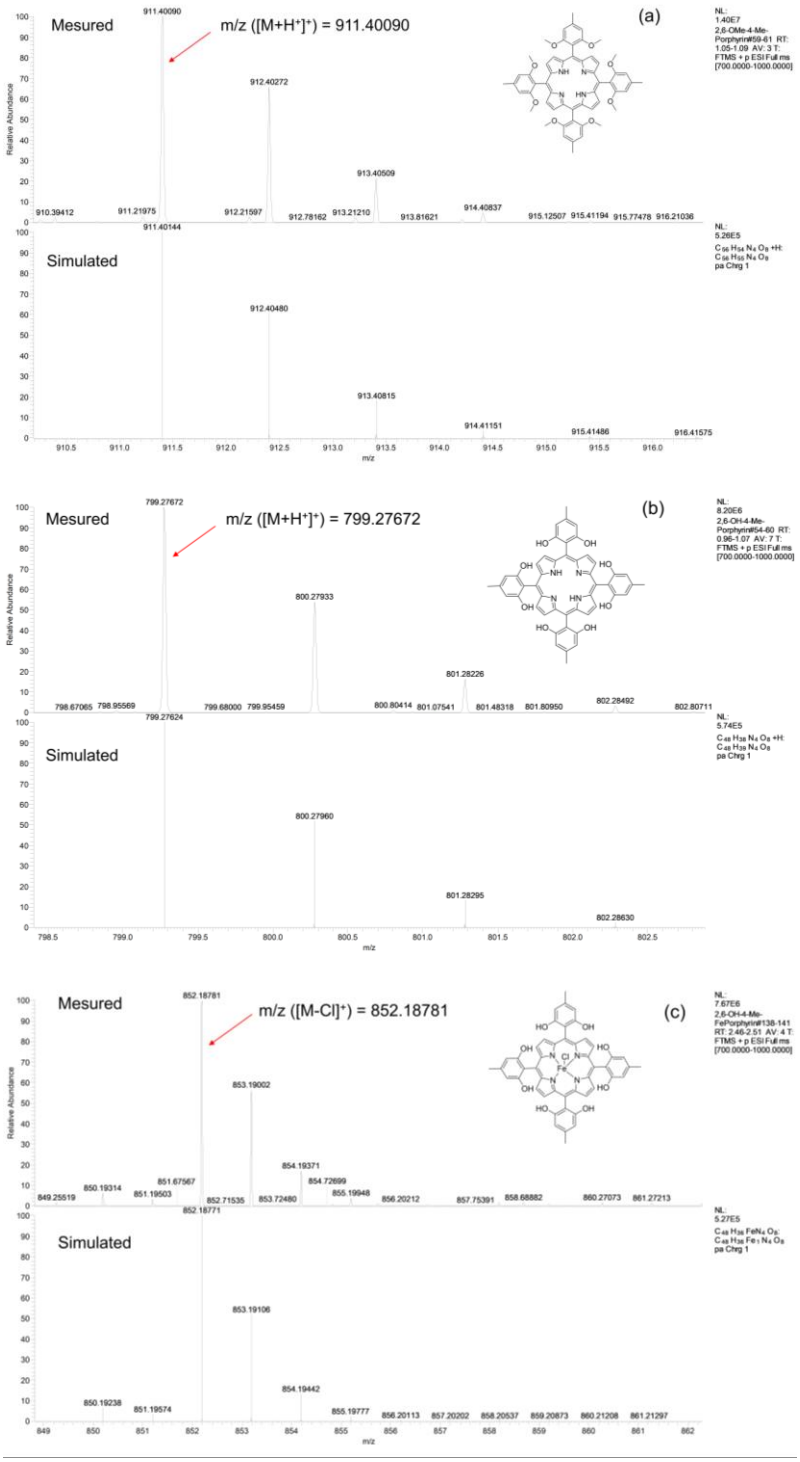

Fig. S8 HRMS spectra of 5, 10, 15, 20-tetrakis(2',6'-dimethoxy-4'-methylphenyl)porphyrin (a); 5, 10, 15, 20-tetrakis(2',6'-dihydroxy-4'-methylphenyl)porphyrin (b); and chloro iron (III) 5, 10, 15, 20-tetrakis(2',6'-dihydroxy-4'-methylphenyl)porphyrin (**Fe3**) (c) in CH_3OH (positive ion mode).

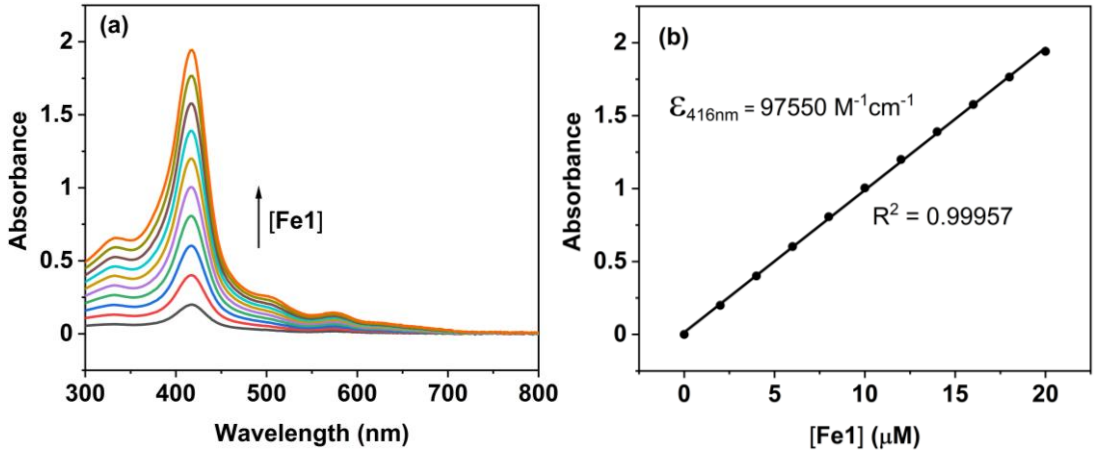

Fig. S9 (a) UV-vis absorption spectra of **Fe1** in DMF at different concentrations. (b) Linear plots of absorbance at 416 nm.

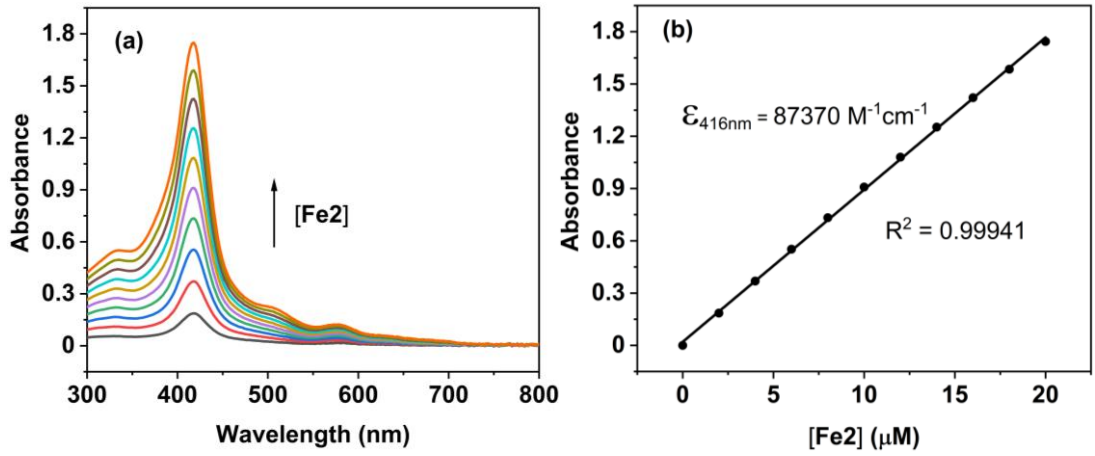

Fig. S10 (a) UV-vis absorption spectra of **Fe2** in DMF at different concentrations. (b) Linear plots of absorbance at 416 nm.

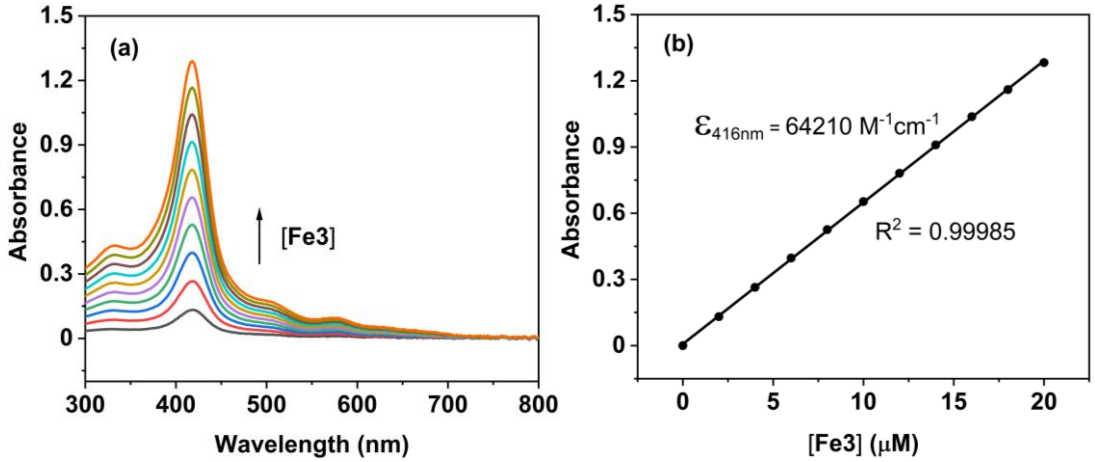

Fig. S11 (a) UV-vis absorption spectra of **Fe3** in DMF at different concentrations. (b) Linear plots of absorbance at 416 nm.

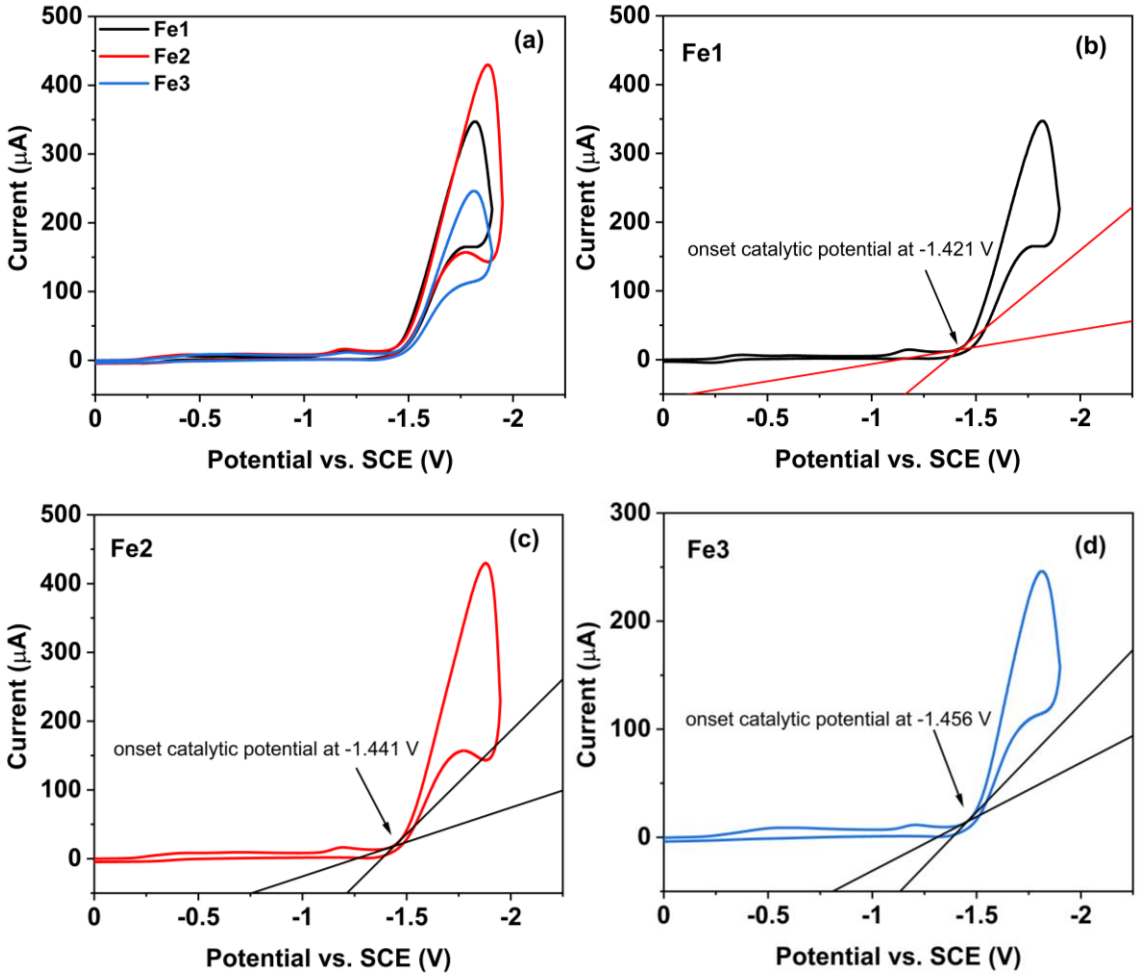

Fig. S12 Cyclic voltammograms of 1.0 mM **Fe1** (black), **Fe2** (red) and **Fe3** (blue) in 5 mL DMF containing 0.1 M $TBAPF_6$ under CO_2 (a), along with the onset of the catalytic potential (b-d).

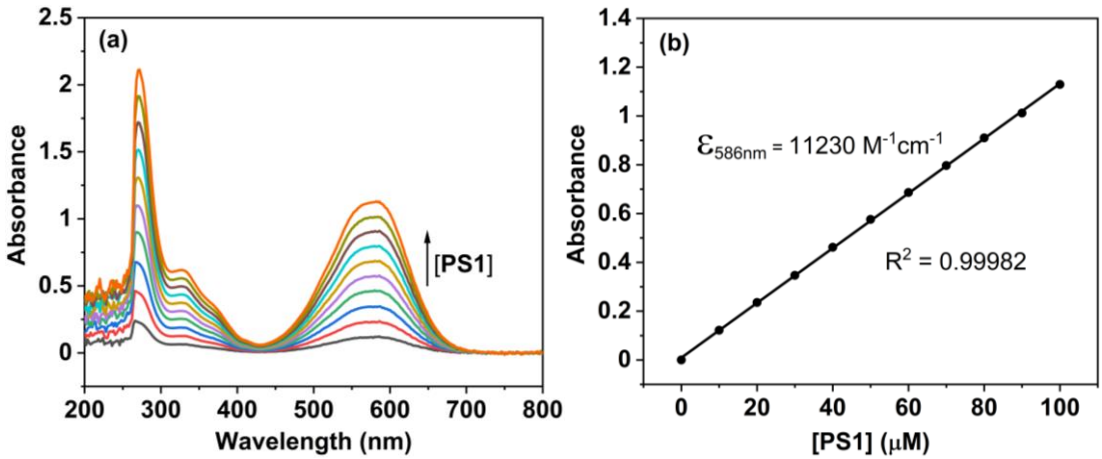

Fig. S13 (a) UV-vis absorption spectra of **PS1** in DMF at different concentrations. (b) Linear plots of absorbance at 586 nm.

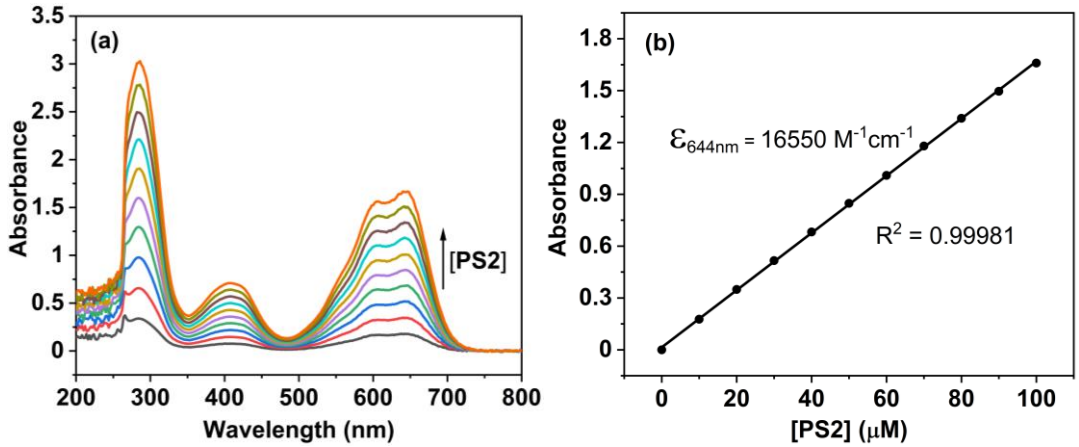

Fig. S14 (a) UV-vis absorption spectra of **PS2** in DMF at different concentrations. (b) Linear plots of absorbance at 644 nm.

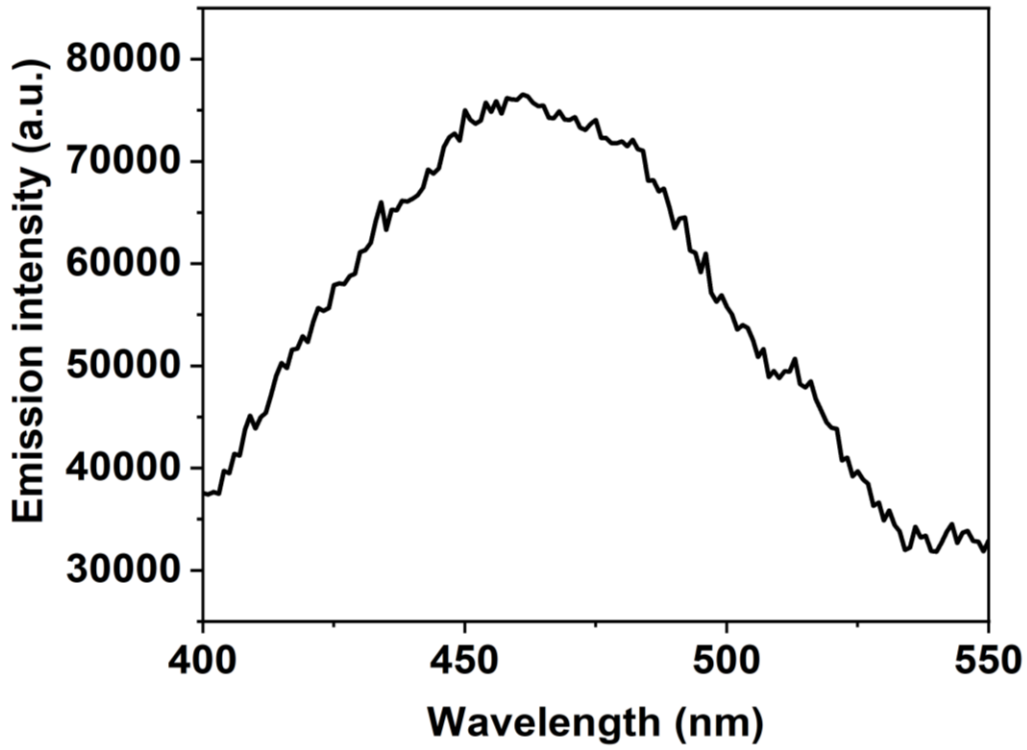

Fig. S15 Excitation spectra (λ_{em}: 600 nm) of **PS1** at 298 K in DMF.

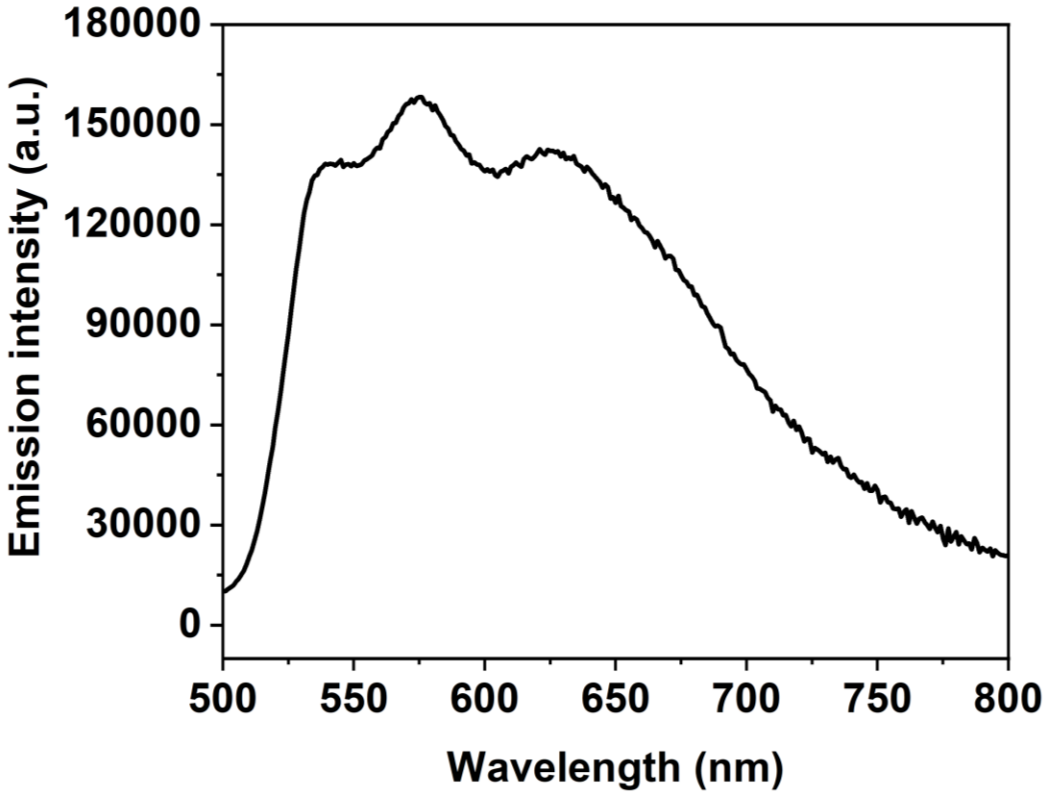

Fig. S16 Emission spectra (λ_{exc}: 460 nm) of **PS1** at 298 K in DMF.

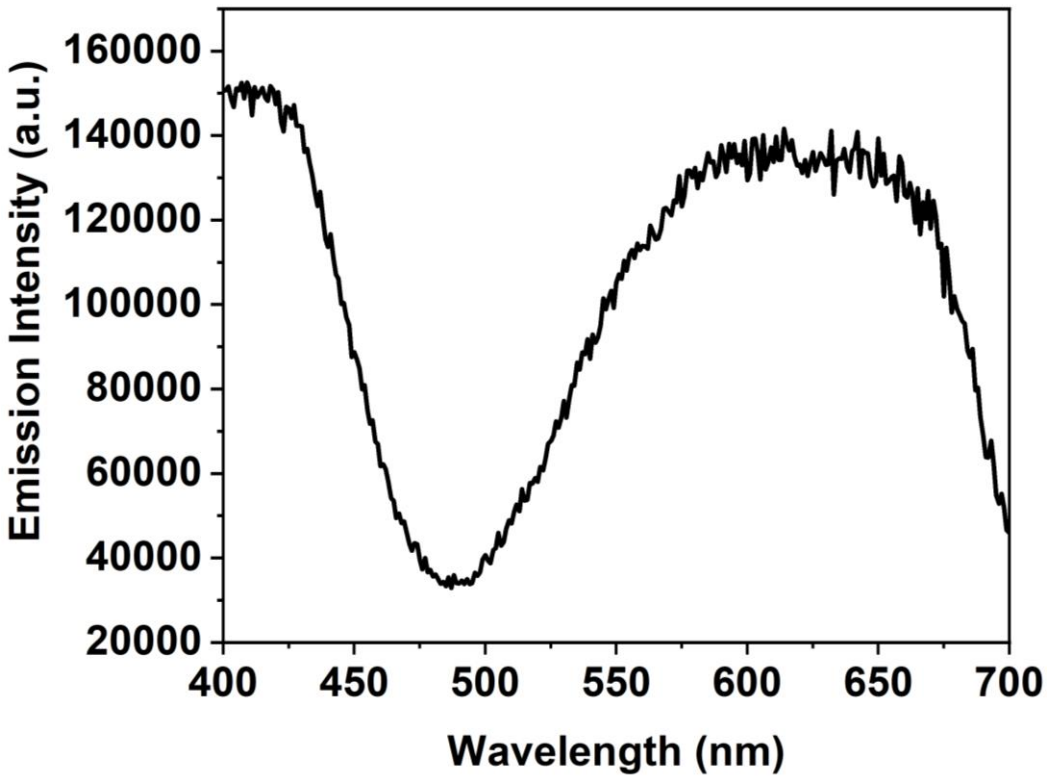

Fig. S17 Excitation spectra (λ_{em}: 750 nm) of **PS2** at 298 K in DMF.

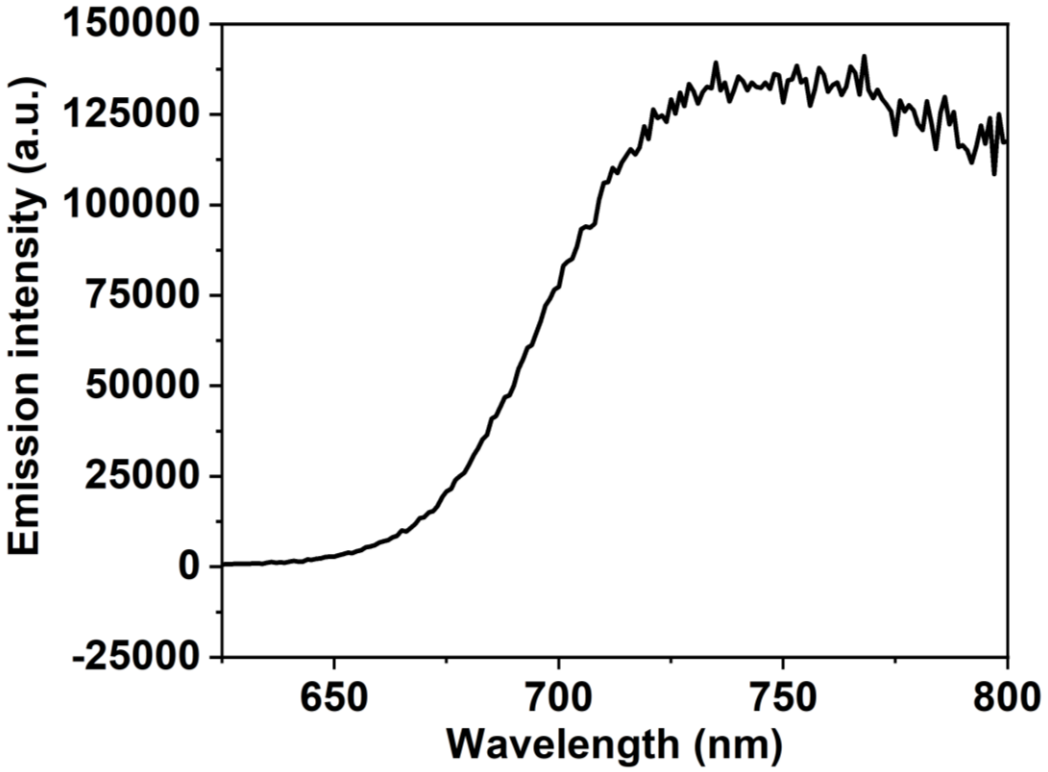

Fig. S18 Emission spectra (λ_{exc}: 600 nm) of **PS2** at 298 K in DMF.

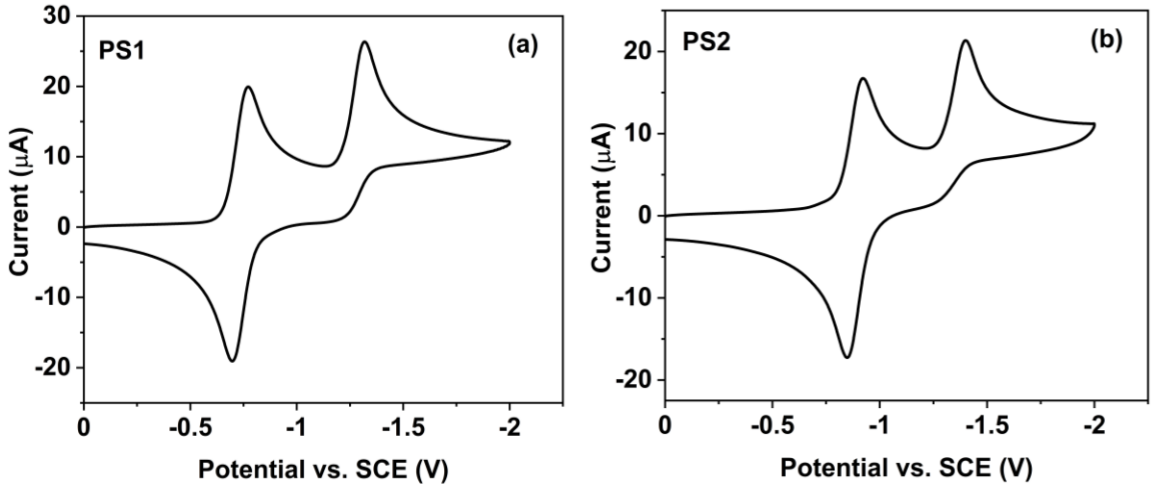

Fig. S19 Cyclic voltammograms of 1.0 mM **PS1** (a) and **PS2** (b) in 5 mL DMF containing 0.1 M $TBAPF_6$ under N_2.

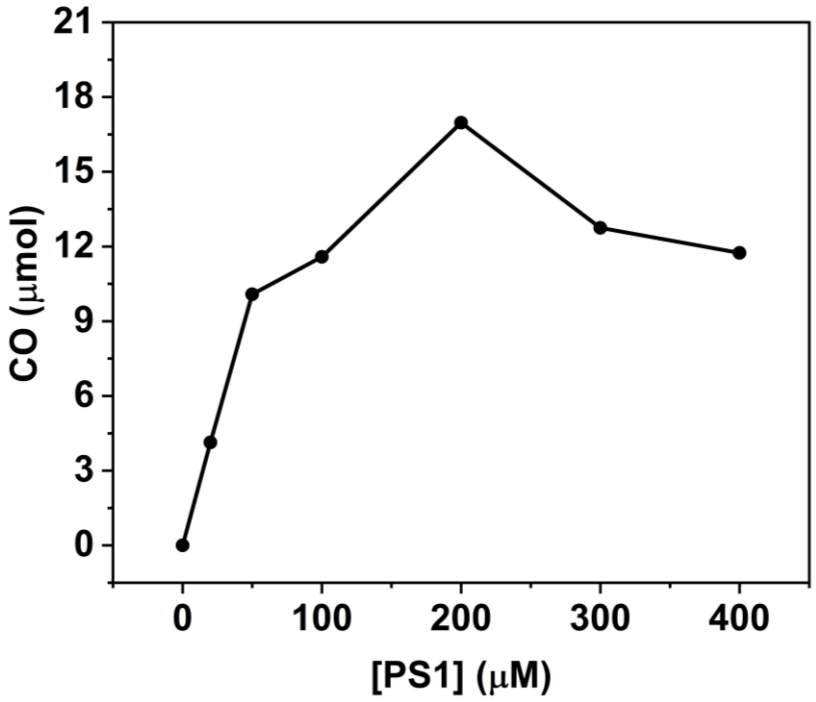

Fig. S20 The amounts of CO of the photocatalytic CO_2 reduction experiments irradiated for 9 h in CO_2-saturated DMF solution containing 1 μM **Fe1** and 10 mM BIH with varying amounts of [**PS1**].

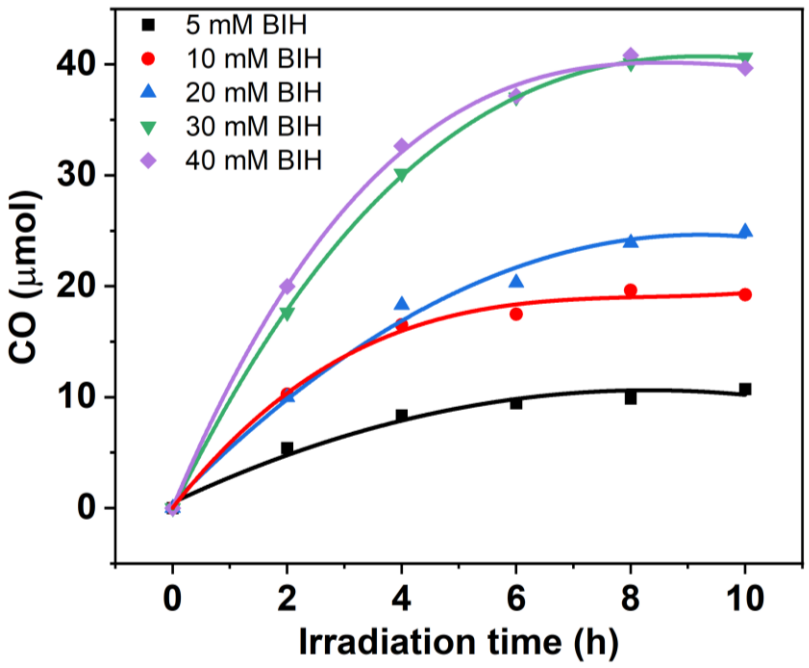

Fig. S21 CO generation in CO_2-saturated DMF solutions containing 1.0 μM **Fe1** and 0.2 mM **PS1** at different BIH concentrations.

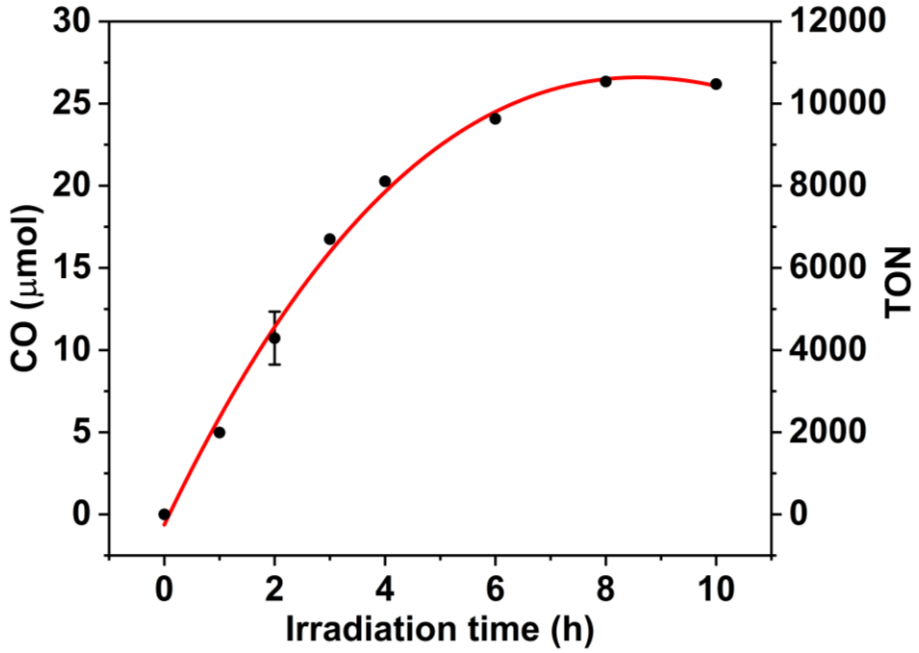

Fig. S22 CO generation in CO_2-saturated DMF solutions containing 0.5 μM **Fe1**, 0.2 mM **PS1**, and 30 mM BIH.

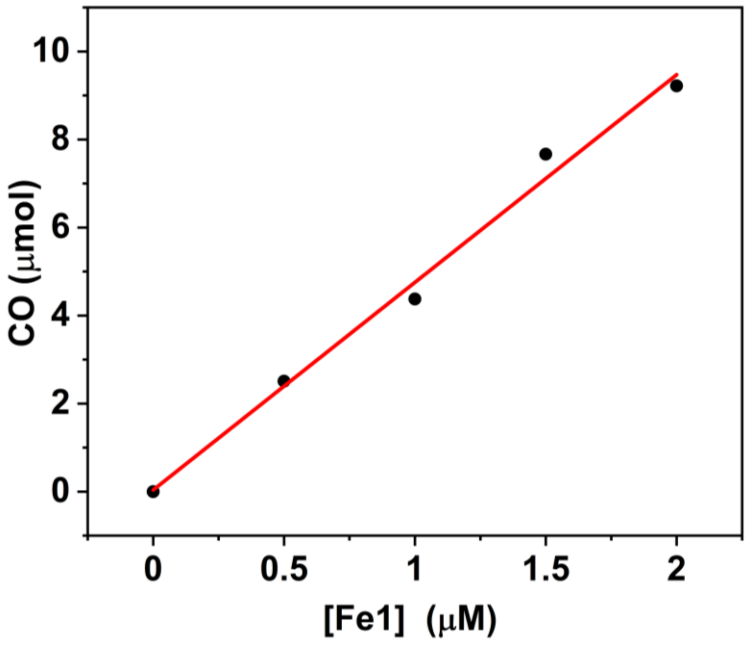

Fig. S23 The amounts of CO of the photocatalytic CO_2 reduction experiments irradiated for 1 h in CO_2-saturated DMF solution containing 200 μM **PS1** and 30 mM BIH with varying amounts of [**Fe1**].

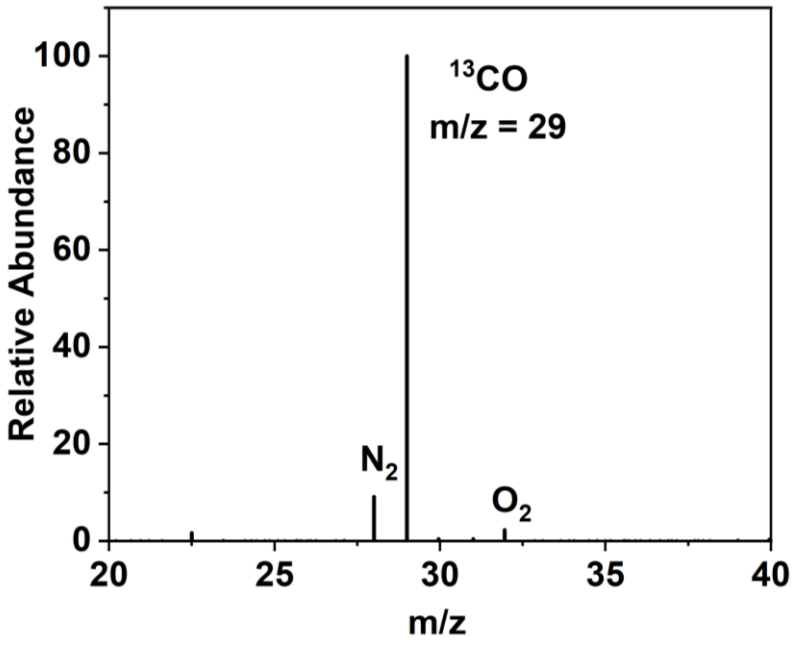

Fig. S24 GC-MS analyses of photocatalytic experiments under $^{13}CO_2$-saturated DMF solutions containing: 30 mM BIH, 1.0 μM **Fe1** and 0.2 mM **PS1**. The small peaks (m/z = 28 and 32) in a ratio of 4:1 are N_2 and O_2 from the air introduced during sample injections.

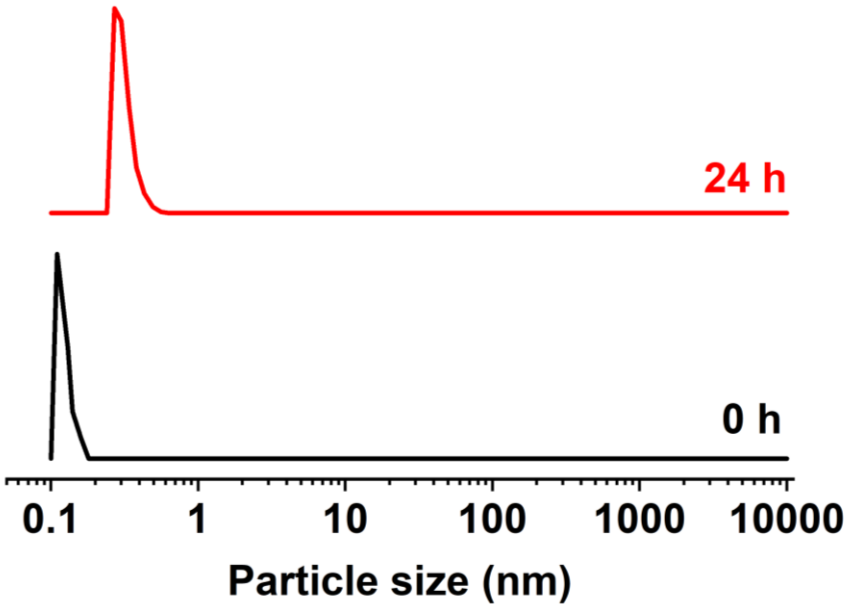

Fig. S25 Particle size distribution of a CO_2-saturated DMF solution containing 0.2 mM **PS1**, 1 μM **Fe1** and 30 mM BIH determined by dynamic light scattering (DLS) measurement before and after irradiation.

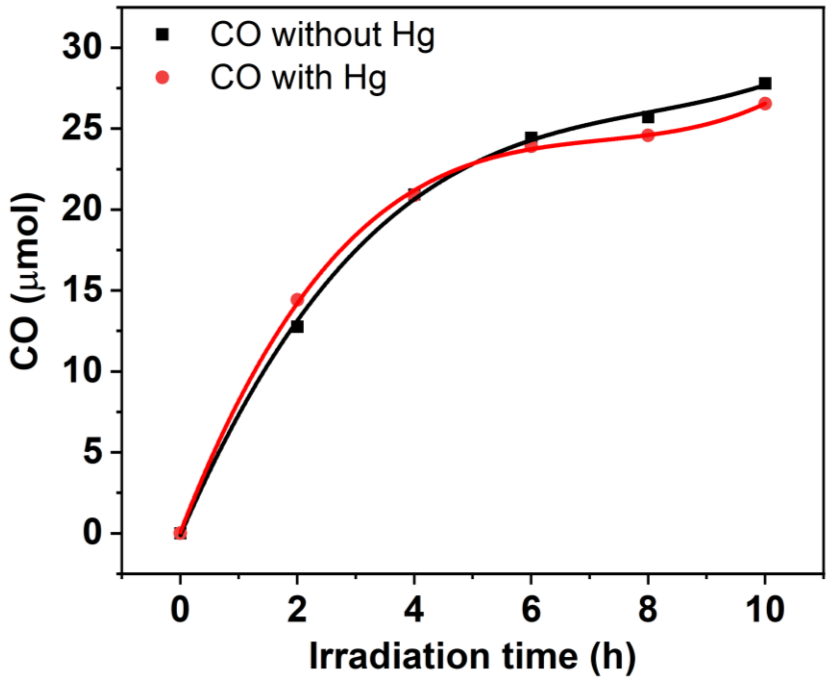

Fig. S26 CO generation in CO_2-saturated DMF solutions containing 10 mM BIH, 1.0 μM **Fe1**, and 0.2 mM **PS1** in the presence and absence of Hg^0 (~0.02 mL) under blue LED.

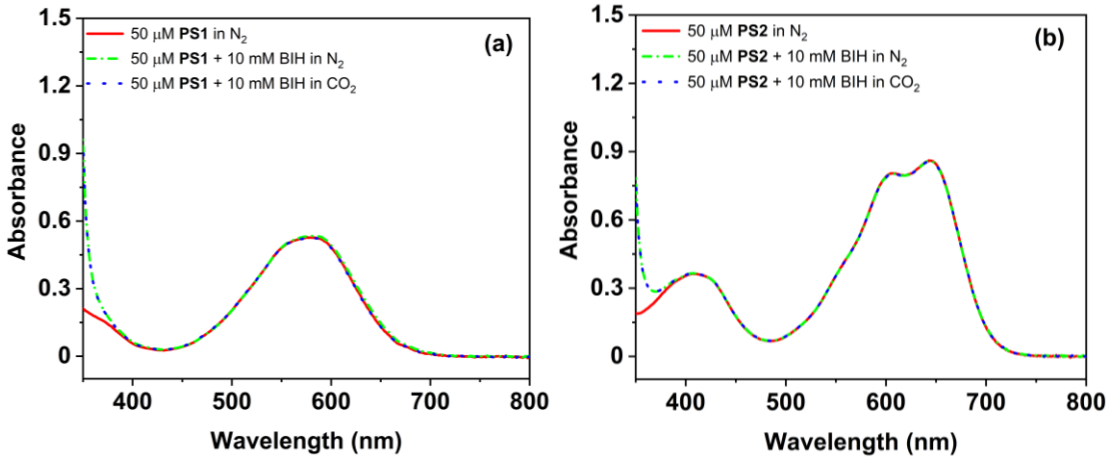

Fig. S27 UV-vis absorption spectra of 50 μM **PS1** (a) and **PS2** (b), with or without the presence of 10 mM BIH in DMF under N_2 and CO_2 at 298 K.

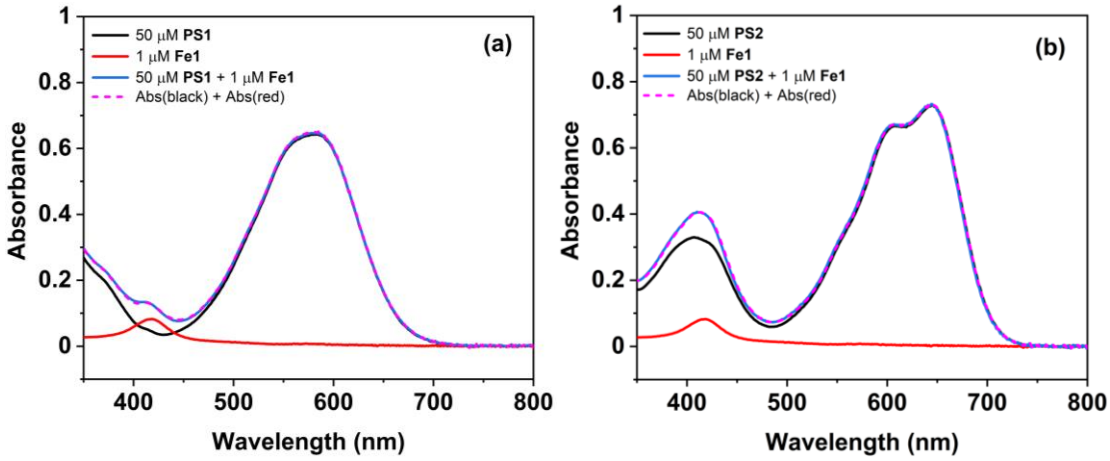

Fig. S28 UV-vis absorption spectra of 50 μM photosensitizer,1 μM **Fe1**, and a mixture of 50 μM photosensitizer and 1 μM **Fe1** in DMF under CO_2 at 298 K.

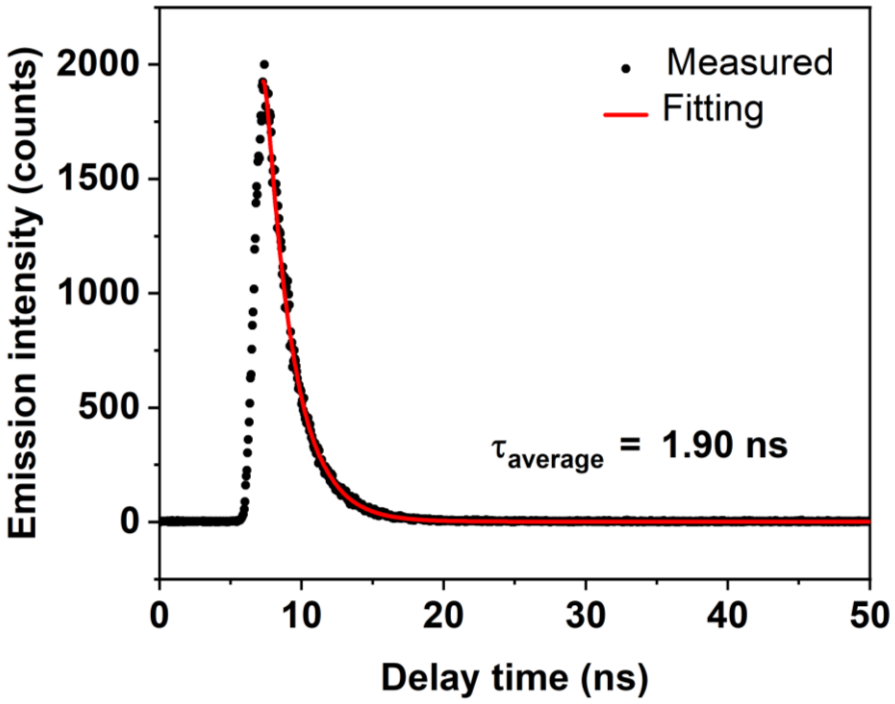

Fig. S29 Emission decay of 50 μM **PS1** in DMF at 298 K. The decay curve was fitted with a double exponential equation ($I(\tau) = A_1exp(-\tau/\tau_1) + A_2exp(-\tau/\tau_2)$).

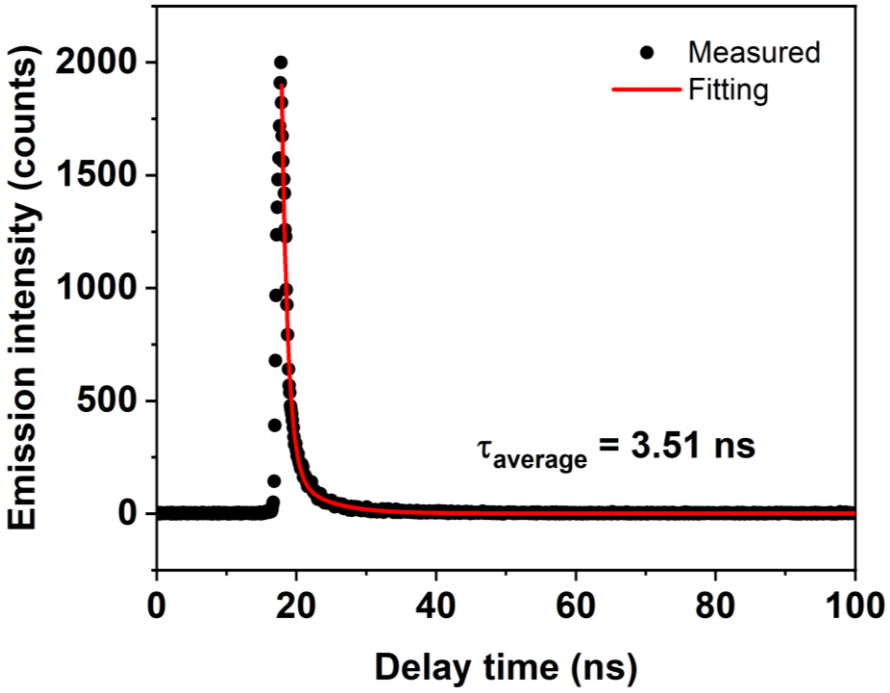

Fig. S30 Emission decay of 50 μM **PS2** in DMF at 298 K. The decay curve was fitted with a double exponential equation ($I(\tau) = A_1exp(-\tau/\tau_1) + A_2exp(-\tau/\tau_2)$).

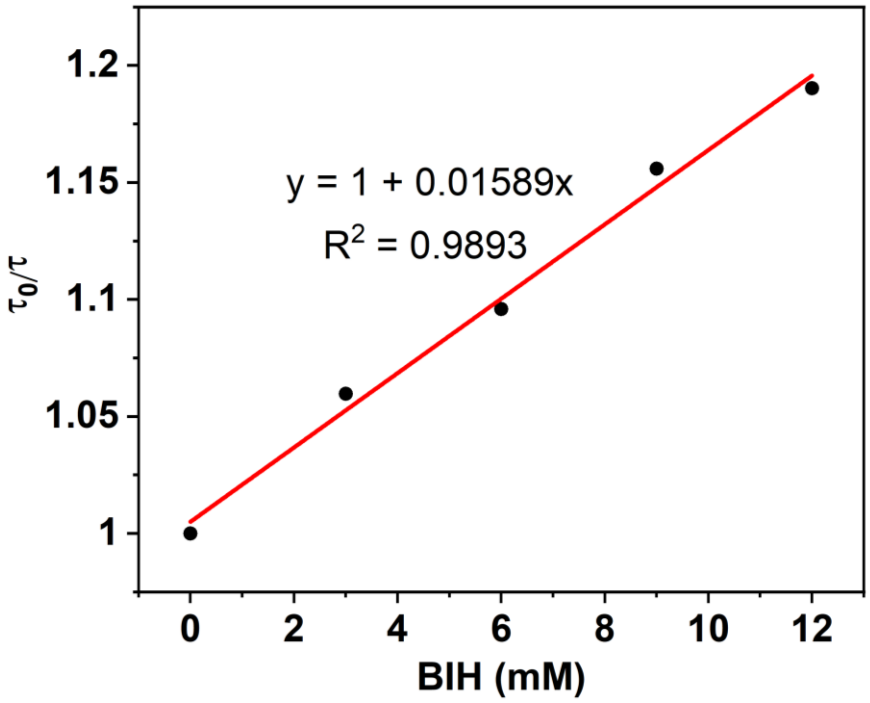

Fig. S31 Stern-Volmer plots of fluorescence lifetime quenching of 50 μM **PS1** in DMF under N_2.

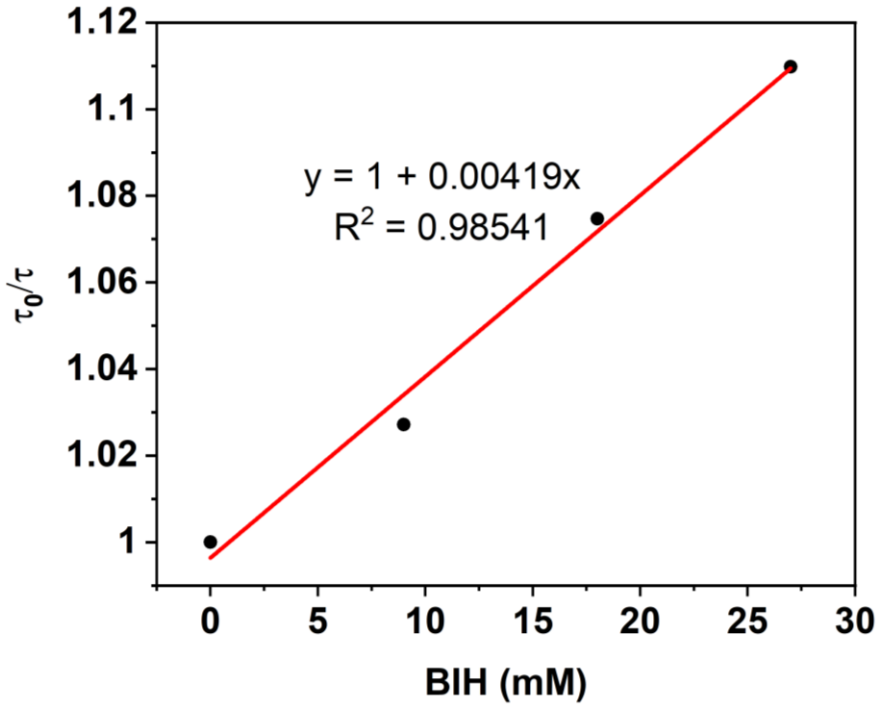

Fig. S32 Stern-Volmer plots of fluorescence lifetime quenching of 50 μM **PS2** in DMF under N_2.

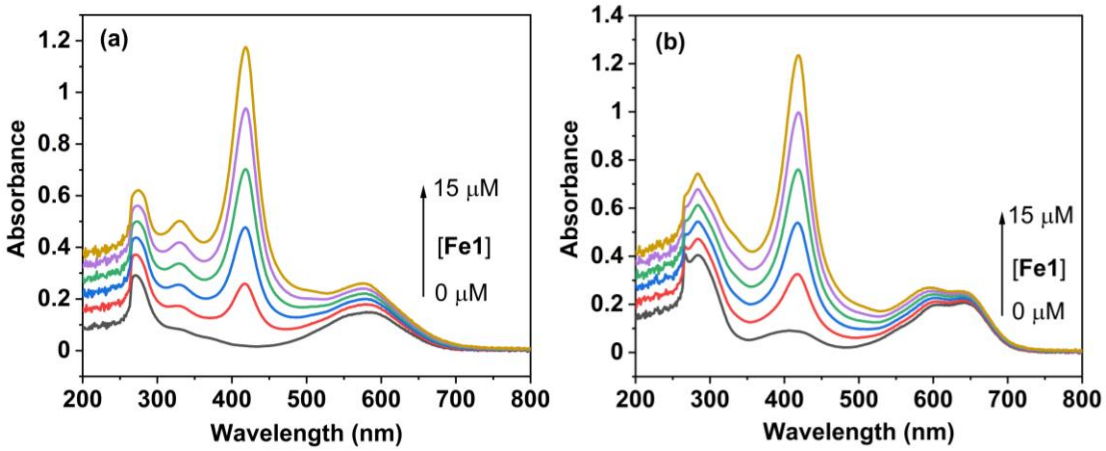

Fig. S33 UV-vis absorption spectra of 20 μM **PS1** (a) and **PS2** (b) in DMF at 298 K with addition of varying amounts of **Fe1**.

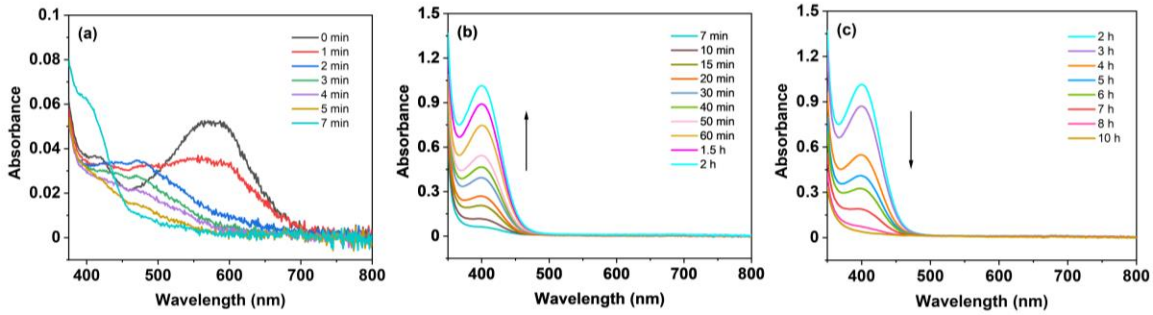

Fig. S34 UV-vis absorption spectra of systems containing 10 mM BIH, 1 μM **Fe1** and 20 μM **PS1** in CO_2-saturated DMF at 298 K under irradiation with a blue LED (λ = 450 nm). Irradiation time ranging from 0 to 7 min (a), from 7 min to 2 h (b), and from 2 to 10 h (c).

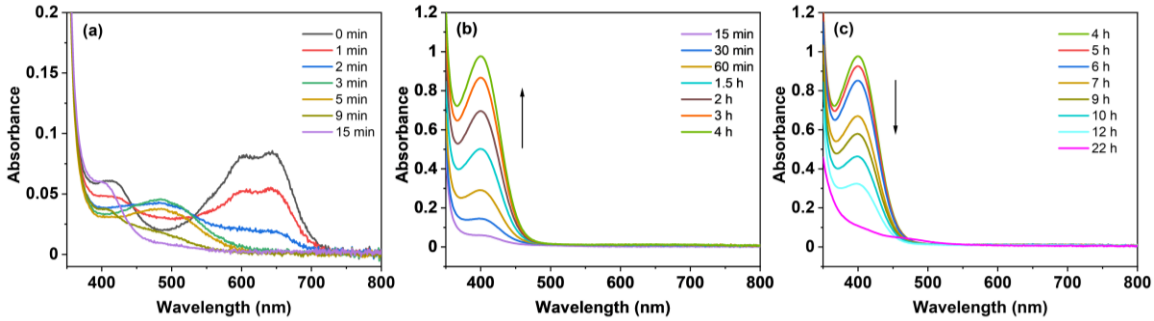

Fig. S35 UV-vis absorption spectra of systems containing 10 mM BIH, 1 μM **Fe1** and 20 μM **PS2** in CO_2-saturated DMF at 298 K under irradiation with a blue LED (λ = 450 nm). Irradiation time ranging from 0 to 15 min (a), from 15 min to 4 h (b), and from 4 to 22 h (c).

Table S1. Electrochemical properties of catalyst under N_2 and CO_2 atmospheres.

Catalyst	$Fe^{III/II}$ (V vs. SCE)[a]	$Fe^{II/I}$ (V vs. SCE)[a]	$Fe^{I/0}$ (V vs. SCE)[a]	Onset catalytic potential (V vs. SCE)[b]
Fe1	-0.29	-1.17	-1.58	-1.42
Fe2	-0.32	-1.16	-1.55	-1.44
Fe3	-0.35	-1.17	-1.60	-1.46

[a]Under N_2 atmosphere; [b]Under CO_2 atmosphere.

Table S2. Photophysical parameters of **PS1** and **PS2** at 298 K in DMF solutions.

Photosentizer	λ_{max} abs/nm (ε M^{-1} cm^{-1})	E_{red} (V vs. SCE)	τ_0 (ns)[a]	k_q (M^{-1} s^{-1})
PS1	586 (11230)	-0.733, -1.28	1.90	8.37×10^9
PS2	644 (16550)	-0.885, -1.35	3.51	1.19×10^9

[a]50 μM photosensitizer, a picosecond pulsed diode laser (λ = 472 nm) was used as the excitation source.

Table S3 Control experiments for photocatalytic CO_2 reduction for 10 h[a]

Entry	Catalyst	Photosensitizer	Electron donor	CO (μmol)	TON_{CO}	Sel_{CO}
1	**Fe1**	**PS1**	BIH	50.3	10052	100
2	**Fe1**	**PS1**	BIH	26.2	10476	100
3	**Fe2**	**PS1**	BIH	25.6	5115	100
4	**Fe3**	**PS1**	BIH	21.5	4305	100
5	**Fe1**	**PS2**	BIH	25.6	5112	100
6	**Fe2**	**PS2**	BIH	17.6	3519	100
7	**Fe3**	**PS2**	BIH	16.6	3330	100
8	**Fe1**	**PS1**	BIH	0	0	N/A
9	**Fe1**	**PS1**	BIH	0	0	N/A
10	**Fe1**	**PS1**	-	0	0	N/A
11	-	**PS1**	BIH	0	0	N/A
12	**Fe1**	-	BIH	0	0	N/A

[a]In a typical photocatalytic experiment, a solution containing 1 μM catalyst, 0.2 mM photosensitizer and BIH (30 mM) was irradiated using blue LED ($\lambda = 450$ nm) for 10 h under a CO_2 atmosphere. Entry 2: 0.5 μM **Fe1**, Entry 8: under N_2, Entry 9: in dark, Entry 10: without BIH, Entry 11: without catalyst, Entry 12: without photosensitizer.

Table S4. The performance of photocatalytic CO_2 reduction with porphyrin complexes in noble-metal-free systems in the literature

Photosensitizer	Catalyst	Solvent	Electron donor	TON_{CO}	TON_{H2}	Φ_{CO}(%)	Sel_{CO}(%)[a]	Light source	Reference
PS1	**Fe1** (0.5 μM)	DMF	BIH	10476	0	0.95	100	blue LEDs (λ = 450 nm)	**This work**
PS1	**Fe2** (1 μM)	DMF	BIH	5115	0	0.63	100		
PS1	**Fe3**(1 μM)	DMF	BIH	4305	0	0.43	100		
1-amino-2-bromo-4-hydroxy-9,10-anthraquinone	**Fe2** (0.6 μM)	DMF	BIH	21616	trace	11.1	>99	White LEDs (λ > 400 nm)	4
CuPP	**Fe2** (0.2 μM)	DMF	BIH	16109	843	6.0	95	White LEDs (λ > 400 nm)	5
9-CNA	**Fe2** (2 μM)	MeCN	TEA	60	0	8×10^{-4}	100	Xe lamp (λ > 400 nm)	6
Non-sensitized	Fe-*p*-TMA (2 μM)	MeCN	BIH	101	0	-	100	solar simulator, 1 sun (λ > 420 nm)	7
Non-sensitized	**Fe2** (10 μM)	MeCN	TEA	30	10	-	75	Xe lamp (cut off IR and low UV)	8
3,7-di(4-biphenyl)-1-naphthalene-10-phenoxazine	Fe-*p*-TMA (10 μM)	DMF	TEA	140	23	-	73	solar simulator, 1 sun (λ > 435 nm)	9
Purpurin	Fe-*p*-TMA (2 μM)	MeCN/H_2O (1:9, v/v)	TEA	60	3	-	95	solar simulator, 1 sun (λ > 420 nm)	10
CuPS	Co(pTMPyP) (5 μM)	0.1 M $NaHCO_3$ buffer	AscHNa	2680	820	1.6	77	Xe lamp (800 > λ > 400 nm)	11

Table S4 (continued)

Photosensitizer	Catalyst	Solvent	Electron donor	TON_{CO}	TON_{H2}	Φ_{CO}(%)	Sel_{CO}(%)[a]	Light source	Reference
CuPS	Co(oTMPyP) (5 μM)	0.1 M $NaHCO_3$ buffer	AscHNa	4000	460	5.7	90	Xe lamp (800 > λ > 400 nm)	12
p-terphenyl	CoPP (50 μM)	MeCN	TEA	62	-	-	66	Xe lamp (λ < 300 nm)	13
p-terphenyl	FePP (50 μM)	MeCN	TEA	42	-	-	38		

References

1. X.-Q. Zhu, M.-T. Zhang, A. Yu, C.-H. Wang and J.-P. Cheng, *J. Am. Chem. Soc.*, 2008, **130**, 2501-2516.
2. C. Costentin, S. Drouet, M. Robert and J.-M. Savéant, *Science*, 2012, **338**, 90-94.
3. M. Ming, H. Yuan, S. Yang, Z. Wei, Q. Lei, J. Lei and Z. Han, *J. Am. Chem. Soc.*, 2022, **144**, 19680-19684.
4. Q. Lei, H. Yuan, J. Du, M. Ming, S. Yang, Y. Chen, J. Lei and Z. Han, *Nat. Commun.*, 2023, **14**, 1087.
5. H. Yuan, B. Cheng, J. Lei, L. Jiang and Z. Han, *Nat. Commun.*, 2021, **12**, 1835.
6. J. Bonin, M. Robert and M. Routier, *J. Am. Chem. Soc.*, 2014, **136**, 16768-16771.
7. H. Rao, J. Bonin and M. Robert, *Chem. Commun.*, 2017, **53**, 2830-2833.
8. J. Bonin, M. Chaussemier, M. Robert and M. Routier, *ChemCatChem*, 2014, **6**, 3200-3207.
9. H. Rao, C.-H. Lim, J. Bonin, G. M. Miyake and M. Robert, *J. Am. Chem. Soc.*, 2018, **140**, 17830-17834.
10. H. Rao, J. Bonin and M. Robert, *ChemSusChem*, 2017, **10**, 4447-4450.
11. X. Zhang, M. Cibian, A. Call, K. Yamauchi and K. Sakai, *ACS Catal.*, 2019, **9**, 11263-11273.
12. X. Zhang, K. Yamauchi and K. Sakai, *ACS Catal.*, 2021, **11**, 10436-10449.
13. T. Dhanasekaran, J. Grodkowski, P. Neta, P. Hambright and E. Fujita, *J. Phys. Chem. A*, 1999, **103**, 7742-7748.